Microelectrode Study of Gallium Deposition from Chlorogallate Melts

Microelectrodes are used to extract thermodynamic, transport, and kinetic data for the gallium trichloride/1-methyl-3-ethylimidazolium chloride room-temperature molten salt that has been used by the authors to form GaAs thin films. The gallium electrodeposition process, which must be understood for the analysis of the GaAs deposition process, is simulated numerically. A plausible gallium deposition mechanism is identified. Microcylinder electrodes are shown to be advantageous for the acquisition of physicochemical constants. Microdisk electrodes are employed to investigate current oscillation phenomena that appear to be related to metal crystallization processes.

Mark W. Verbrugge
Michael K. Carpenter
Physical Chemistry Department
General Motors Research Laboratories
Warren, MI 48090

Introduction

The analysis of transport and kinetic mechanisms in electrochemical processes constitutes an important step toward the realization of numerous technologies; this is particularly true of electrodeposition processes that can be employed in the fabrication of thin films. For deposition processes, however, the tools required for a complete chemical description are still evolving. Microelectrodes have recently been shown to be superior for the analysis of electrochemical charge-transfer processes (Wightman, 1981; Fleischmann et al., 1987). The following advantages can be identified:

- The ohmic drop is reduced
- Capacitive currents due to electric double layers are reduced
- Transport is enhanced due to spherical diffusion and migration processes
- Small electrolyte volumes can be utilized
- For gas-evolving reactions, gas bubbles do not form even at high current densities
- For costly electrode materials, only small amounts of the electrode material are required

The reduction of ohmic and capacitive effects, coupled with the ability of microelectrodes to obtain high flux rates without observing significant mass-transport resistance, makes microelectrodes ideal for measuring interfacial charge transfer rate constants; that is, the majority of the measured potential drop can be attributed to charge transfer resistance, which allows for a more accurate measurement of the associated rate constants.

In this work, we solve nonlinear transport equations (Newman, 1973a; Bard and Faulkner, 1980) for all mobile species in our chlorogallate electrolyte. In most electroanalytical studies, migration is not addressed (Bamford and Compton, 1986, p. 123). We develop general models for cylindrical and hemispherical electrodes; diffusion and migration are treated numerically, without further approximation. Such a treatment is feasible for these systems since they maintain a uniform reaction distribution, and the transport equations are one-dimensional. The model results are compared with those for the traditional infinite-plane geometry. Controlled-current and controlled-potential experiments for Ga deposition from a room-temperature chlorogallate melt that has been used by the authors to electrodeposit GaAs (Carpenter and Verbrugge, 1989) are analyzed to facilitate an understanding of the complex chemistry associated with this system. Such an understanding is necessary for the intelligent design of a process for the formation of large-area thin films of GaAs, which would be of great technical importance (Frensley, 1987). Migration of the reactants leading to Ga deposition is shown to be an important mode of transport in the analysis.

Before proceeding with a description of the chemistry of the melt system, it is helpful to note relative attributes of the various electrode geometries typically used for electroanalytical investigations; it was through such an analysis that the authors chose the microcylinder electrodes for this study. Traditionally, electrochemical charge transfer reactions have been studied with stationary planar and rotating-disk electrodes (Bard and Faulkner, 1980; Bamford and Compton, 1986). Dropping-mercury electrodes have also been shown to be practical for many systems, provided that the mercury surface does not

Correspondence concerning this paper should be addressed to M. W. Verbrugge.

significantly alter the system chemistry. Unless special provisions are employed, and they usually are not because of experimental difficulties, planar electrodes maintain a highly nonuniform reaction or current distribution. The same is true of the reaction distribution on a rotating disk operated below the transport-limited current (Newman, 1966b). Integral transform techniques have been used to model transient diffusion to stationary disk electrodes for simplified boundary conditions (constant flux or concentration conditions) (Oldham, 1981; Aoki and Osteryoung, 1981 and 1984; Aoki et al., 1984; Fleischmann and Pons, 1988). In addition, integral-transform techniques for the steady-state, stationary-disk system (Watson, 1952; Carslaw and Jaeger, 1959; Nanis and Kesselman, 1971; Newman, 1973b) have received renewed interest for the simulation of steady-state ionic diffusion to microdisk electrodes (Bond et al., 1988; Fleischmann et al., 1989). The integral-transform techniques are computationally efficient, but can be used only to solve linear equations; therefore migration effects generally cannot be addressed. Transient, two-dimensional reaction distributions on microdisk electrodes (in the absence of migration effects) have been studied numerically by Flanagan and Marcoux (1973) and by Heinze (1981). Aoki and Osteryoung (1981) have compared the various microdisk studies prior to 1981. Carlin and Osteryoung (1988) have recently used microdisk electrodes to investigate the room-temperature chloroaluminate melt, which is discussed below. The mathematical difficulties associated with the two-dimensional microdisk system have prompted electroanalytical researchers to investigate microcylinder electrodes (Stephens and Moorhead, 1984; Kovach et al., 1985; Aoki et al., 1985; Sujaritvanichpong, 1986; Amatore et al., 1986; 1988). Microcylinder electrodes were used in the quantitative electroanalytical work of this study because they observe all of the advantages cited above for microelectrodes and they can be described mathematically by one-dimensional treatments. The primary disadvantage associated with microcylinder electrodes is that transient equations must be solved. The application of microelectrodes to specific chemical systems can be found in recent reviews (Wightman, 1981; Howell, 1987; Fleischmann et al., 1987).

The room-temperature melt is formed by combining solid 1-methyl-3-ethylimidazolium chloride (ImCl) with solid gallium trichloride, which results in an exothermic reaction that yields a liquid phase. Based on the known chemistry of the $AlCl_3$–ImCl system (Hussey, 1983), it is likely that the $GaCl_3$ accepts a chloride anion separated from the ImCl species, forming $GaCl_4^-$:

$$GaCl_3 + (Im^+ \cdots Cl^-) \rightleftharpoons GaCl_4^- + Im^+ \qquad (1)$$

with equilibrium constant K_I. The $GaCl_4^-$ species can further react with any free $GaCl_3$ to form $Ga_2Cl_7^-$:

$$GaCl_4^- + GaCl_3 \rightleftharpoons Ga_2Cl_7^- \qquad (2)$$

with equilibrium constant K_{II}. Initial experimental studies of the $GaCl_3$–ImCl melt have been recently published (Wicelinski and Gale, 1987; Wicelinski et al., 1987). Since very little $GaCl_3$ is thought to exist in the melts, it is expedient to combine Eqs. 1 and 2 to obtain the following expression for the dimerization reaction

$$2GaCl_4^- \underset{k_b}{\overset{k_f}{\rightleftharpoons}} Ga_2Cl_7^- + Cl^- \qquad (3)$$

with equilibrium constant K_{III}. Equations 1–3 can be related by

$$K_{III} = \frac{K_{II}}{K_I} \qquad (4)$$

$$= \frac{k_f}{k_b} \qquad (5)$$

where k_f and k_b are forward and backward rate constants, respectively. Hussey et al. (1986) have analyzed the chloroaluminate equilibria using Eq. 3 (replacing Ga with Al) to simulate $AlCl_3$–ImCl concentration cells. They found that K_{III} is $\sim 10^{-16}$ for the aluminum system.

The work of Lai and Skyllas-Kazacos (1988) (and other researchers noted in their references) indicates that for Al deposition from the $AlCl_3$–ImCl melt, the following charge transfer reaction takes place:

$$Al_2Cl_7^- + 3e^- \rightleftharpoons Al + AlCl_4^- + 3Cl^- \qquad (6)$$

It is believed that the $AlCl_4^-$ species is too stable to be reduced, and that only the reduction of the $Al_2Cl_7^-$ species can lead to Al deposition. Since very little chloride ion is present in acidic melts (melts containing molar ratios of $AlCl_3$:ImCl that are greater than unity), reflected by the small value of K_{III} in these melts, the equilibrium expression $2AlCl_4^- \rightleftharpoons Al_2Cl_7^- + Cl^-$ is often combined with Eq. 6 to yield:

$$4Al_2Cl_7^- + 3e^- \rightleftharpoons Al + 7AlCl_4^- \qquad (7)$$

for acidic chloroaluminate melts. We note that this equation implies that a transport-limited current density will not be observed, since through the dimerization reaction there is, effectively, an infinite quantity of the $Al_2Cl_7^-$ dimer. Since transport limitations are known to occur in the aluminum system, and we also observe them in the current work, we take into account the resistance associated with the homogeneous reaction, and we do not use Eq. 7. It is generally postulated that Al reduction does not take place from the basic $AlCl_3$–ImCl melt because no appreciable amounts of $Al_2Cl_7^-$ exist. Since Ga deposits can be formed from basic $GaCl_3$–ImCl (Carpenter and Verbrugge, 1989), we hypothesize that $Ga_2Cl_7^-$ is present in these basic melts, and the following expression is used to describe the Ga deposition process

$$Ga_2Cl_7^- + 3e^- \rightleftharpoons Ga + GaCl_4^- + 3Cl^- \qquad (8)$$

Equations 3 and 8 constitute our description of the salient chemistry of the Ga deposition process from the $GaCl_3$–ImCl melt.

Experimental Studies

Materials

The electrolyte was a room-temperature molten salt consisting of gallium trichloride (Johnson Matthey, 99.999%) and

1-methyl-3-ethylimidazolium chloride with a molar ratio of 40:60. The synthesis of the organic chloride and the melt have been described previously (Carpenter and Verbrugge, 1989). Microdisk electrodes, obtained from Bioanalytical Systems, Inc., consisted of 5 μm radius Pt disks potted in an inert chlorofluorocarbon polymer (Kel-F). Microcylinder electrodes were fabricated by sealing a Pt wire (Johnson Matthey), 12.5 μM in radius, in a glass pipette such that approximately 0.5 cm of the wire was exposed. A small amount of mercury was placed in the pipette to provide electrical contact to a thicker Pt wire lead which was subsequently sealed with silicon sealant into the opposite end of the pipette, as shown in Figure 1. An aluminum wire reference electrode (Alfa) was briefly dipped in nitric acid and rinsed with purified water prior to use.

Instrumentation and Cell Design

All experiments were performed at ambient temperature, approximately 22°C, in a Vacuum Atmospheres glove box (model DLX-001-S-P) containing dry nitrogen (99.9995% N_2, Scott Specialty Gases). The experimental cell, described previously (Carpenter and Verbrugge, 1989), consisted of a three-electrode setup with the aluminum reference electrode located in a remote cell compartment to prevent aluminum contamination of the electrolyte. Microelectrode experiments were conducted without stirring. Potential or galvanostatic control of the cell electrodes was provided by an EG&G Princeton Applied Research Potentiostat/Galvanostat model 273. A Nicolet 4094B digital storage oscilloscope was used to collect the data for storage on floppy disks. Data analysis and display were performed on an IBM PC/AT using software developed by S-Cubed (a division of Maxwell Laboratories).

Mathematical Model

In this section, a mathematical model is presented that can be used to describe Ga deposition from a $GaCl_3$/ImCl molten-salt electrolyte. The relevant phenomenological equations are presented first, followed by the conservation equations required to satisfy the natural laws of classical physics.

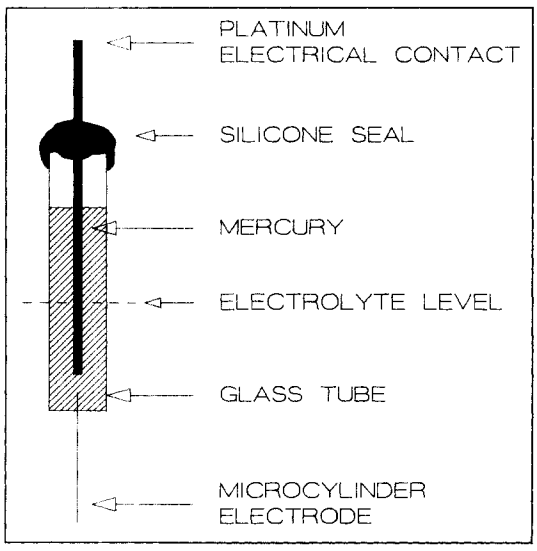

Figure 1. Microcylinder electrode.

Models for transport in concentrated solutions such as our melt system all contain an unsatisfying degree of approximation since it is impossible to take into account all of the multibody interactions. The Stefan-Maxwell approach (Hirschfelder et al., 1954) has become one of the more accepted approaches. To use the Stefan-Maxwell approach is probably not warranted in this initial study of the chlorogallate melt. We employ a simpler analysis that makes use of a Nernst-Planck ionic flux equation. The Stefan-Maxwell approach is more rigorous, although it too is approximate, and more parameters (six binary-interaction coefficients for our four-species system) are introduced that we do not presently have a good way of estimating. To indicate the approximations inherent in our analysis, we begin by writing the electrochemical potential μ_i of an ion i as

$$\mu_i = \mu_i^o + RT \ln c_i \Gamma_i + z_i F \Phi$$

where μ^o represents a standard state, R is the gas constant, T is temperature, c is concentration, Γ is an activity coefficient, z is a charge number, F is Faraday's constant, and Φ is the electric potential. We now specify that electrical contributions to μ_i enter only through the last term. (A critical discussion of such a definition for μ_i can be found in Newman, 1973a.) All other contributions are termed chemical. We now write the flux N_i in terms of the gradient in μ_i

$$N_i = -\frac{D_i}{RT} c_i \nabla \mu_i$$

This equation can be viewed as a definition of D_i. Upon substituting in our expression for μ_i, we obtain

$$N_i = -D_i \nabla c_i - z_i F \frac{D_i}{RT} \nabla \Phi - D_i c_i \nabla \ln \Gamma_i$$

If the activity coefficient is not a function of position, $\nabla \ln \Gamma_i = 0$ (implying that all species are chemically similar), and the Nernst-Planck equation results:

$$N_i = -z_i F \frac{D_i}{RT} c_i \nabla \Phi - D_i \nabla c_i \tag{9}$$

The following subscript convention will be used to refer to the various species

1	Im^+
2	$GaCl_4^-$
3	$Ga_2Cl_7^-$
4	Cl^-

The rate of the homogeneous reaction yielding $Ga_2Cl_7^-$, Eq. 3, is represented by

$$R_3 = k_f c_2^2 - k_b c_3 c_4 \tag{10}$$

The rate constants for this reaction, k_f and k_b, are related to the equilibrium constant K_{III} by Eq. 5.

The Butler-Volmer equation (Newman, 1973a; Bard and Faulkner, 1980) constitutes the final phenomenological equa-

tion employed. For the reduction of $Ga_2Cl_7^-$, in accordance with Eq. 8,

$$r_e = \frac{i}{nF} = k_a c_2 c_4^3 \exp[(1-\beta)nf(V-\Phi_o)] - k_c c_3 \exp[(-\beta nf(V-\Phi_o)] \quad (11)$$

where r_e is the rate of the charge-transfer reaction (mol/cm^2 · s); k_a and k_c are the anodic and cathodic rate constants, respectively; n is the number of electrons in the electrochemical reaction (three for gallium deposition); $f = F/(RT)$, a constant under isothermal conditions; β is the symmetry factor ($0 < \beta < 1$); V is the potential of the working electrode measured against a chosen reference (an aluminum wire in this study); and Φ_o is the value of the electric potential in solution just outside the region in which the charge-transfer reaction takes place. The rate constants are related by the equilibrium electrode potential U^o

$$U^o = \frac{RT}{nF} \ln \frac{k_c}{k_a} \quad (12)$$

Equivalent to Eq. 11, the Butler-Volmer equation can be stated as

$$i = i_o \{\exp[(1-\beta)nf\eta_s] - \exp(-\beta nf\eta_s)\} \quad (13)$$

in which i_o is the exchange current density

$$i_o = nFk_c^{(1-\beta)} k_a^{\beta} c_2^{\beta} c_3^{(1-\beta)} c_4^{3\beta} \quad (14)$$

Surface concentrations are employed in Eqs. 11 and 14. The surface overpotential, η_s, reflects the amount of energy devoted to an electrochemical reaction:

$$\eta_s = V - V_e \quad (15)$$

where V_e is the electrode potential difference in the absence of resistance to the charge-transfer reaction. Equations 9, 10, and 11 are the only phenomenological equations employed in the model. A schematic illustration of the electrochemical system and the mathematical analog is given in Figure 2.

Mass and energy conservation equations are utilized in conjunction with Eqs 9, 10, and 11 to complete the mathematical model. Material balances on the $GaCl_4^-$, $Ga_2Cl_7^-$, and Cl^- species yield:

$$\frac{\partial c_2}{\partial t} = z_2 F u_2 (c_2 \nabla^2\Phi + \nabla c_2 \cdot \nabla\Phi) + D_2 \nabla^2 c_2 - 2(k_f c_2^2 - k_b c_3 c_4) \quad (16)$$

$$\frac{\partial c_3}{\partial t} = z_3 F u_3 (c_3 \nabla^2\Phi + \nabla c_3 \cdot \nabla\Phi) + D_3 \nabla^2 c_3 + k_f c_2^2 - k_b c_3 c_4 \quad (17)$$

$$\frac{\partial c_4}{\partial t} = z_4 F u_4 (c_4 \nabla^2\Phi + \nabla c_4 \cdot \nabla\Phi) + D_4 \nabla^2 c_4 + k_f c_2^2 - k_b c_3 c_4 \quad (18)$$

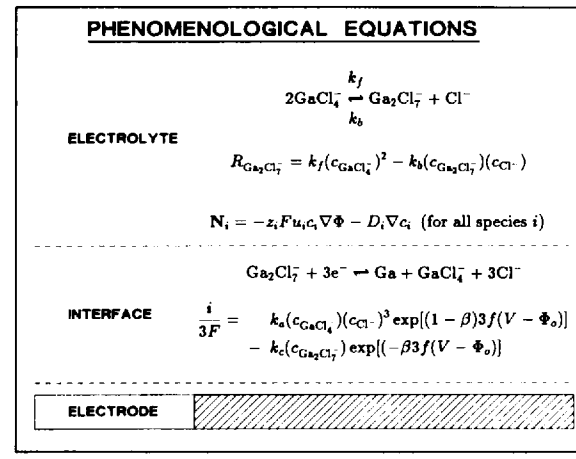

Figure 2. Electrochemical system and mathematical analog.

$u_i = D_i/(RT)$

Listed phenomenological equations are combined with mass and energy conservation equations to complete the model.

Conservation of charge results in two more equations. Electroneutrality is employed so as to eliminate the application of another material balance equation for the Im^+ species

$$\sum_{i=1}^{4} z_i c_i = 0 \quad (19)$$

Secondly, the transport of ions is related to the current density in solution

$$i = F \sum_{i=1}^{4} z_i N_i \quad (20)$$

which can be combined with Eq. 9 to state

$$\nabla\Phi = -\frac{i + F\sum_{i=1}^{4} z_i D_i \nabla c_i}{F^2 \sum_{i=1}^{4} z_i^2 \frac{D_i}{RT} c_i} \quad (21)$$

where the denominator is the conductivity of the electrolyte κ.

The five unknowns (c_i and Φ) can be obtained by solution of the field equations, Eqs. 16–19 and 21. The initial conditions are that of bulk concentration for all species ($c_i = c_i^{\infty}$). The bulk concentrations can be obtained as follows. First, it is recognized that the $GaCl_3$ added initially to the ImCl reacts to form $GaCl_4^-$ and $Ga_2Cl_7^-$

$$c_{GaCl_3} = c_2^{\infty} + 2c_3^{\infty} \quad (22)$$

Second, in accordance with Eq. 3,

$$c_3^{\infty} = K_{III} \frac{(c_2^{\infty})^2}{c_4^{\infty}} \quad (23)$$

Last, electroneutrality must be observed, which provides the third equation for the three unknown bulk concentrations; c_2^{∞},

c_3^∞, and c_4^∞. The concentration of the imidazolium cation c_1^∞ is simply calculated from the amount of ImCl added initially. For c_4^∞, the following equation is easily solved by Newton's method (Conte and de Boor, 1980)

$$0 = -\frac{\sqrt{1 + 4(2K_{III}/c_4^\infty)} - 1}{2(2K_{III}/c_4^\infty)c_{GaCl_3}} - \frac{K_{III}}{c_4^\infty}\left[\frac{\sqrt{1 + 4(2K_{III}/c_4^\infty)c_{GaCl_2}} - 1}{2(2K_{III}/c_4^\infty)}\right]^2 - c_4^\infty + c_1^\infty \quad (24)$$

Upon solution of this equation for c_4^∞, the following two equations can be utilized to obtain c_2^∞ and c_3^∞:

$$c_2^\infty = \frac{\sqrt{1 + 4(2K_{III}/c_4^\infty)c_{GaCl_3}} - 1}{2(2K_{III}/c_4^\infty)} \quad (25)$$

$$c_3^\infty = \frac{K_{III}}{c_4^\infty}\left(\frac{\sqrt{1 + 4(2K_{III}/c_4^\infty)c_{GaCl_3}} - 1}{2(2K_{III}/c_4^\infty)}\right)^2 \quad (26)$$

The boundary conditions far from the electrode are

$$c_i(t, \infty) = c_i^\infty \ (i = 1, 2, 3, 4) \quad (27)$$

$$\Phi(\infty) = 0 \quad (28)$$

At the electrode surface, the species fluxes and concentrations are related to the charge transfer reaction rate by means of the cell current density:

$$-\left.\frac{i}{nF}\right|_{r=a} = -z_2Fu_2c_2\nabla\Phi - D_2\nabla c_2 \quad (29)$$

$$\left.\frac{i}{nF}\right|_{r=a} = -z_3Fu_3c_3\nabla\Phi - D_3\nabla c_3 \quad (30)$$

$$-\left.\frac{3i}{nF}\right|_{r=a} = -z_4Fu_4c_4\nabla\Phi - D_4\nabla c_4 \quad (31)$$

where a is the electrode radius for microhemisphere and microcylinder electrodes, and 0 for planar electrodes. (Equations 19 and 21 can be applied as they are written at the electrode surface.)

For controlled-current experiments (chronopotentiometry), the species concentrations and fluxes are independent of the electrode potential V, provided only one electrochemical reaction takes place, and the reaction rate is uniform over the electrode surface (as is the case for the microcylinder and microhemisphere electrodes). For controlled-potential experiments (chronoamperometry), a current-potential-concentration relationship (for example, the Butler-Volmer equation, Eq. 11) is applied to obtain the cell current. It is clear that for one-dimensional systems, controlled-current processes are easier to simulate than controlled-potential processes, as has been noted previously (Verbrugge and Tobias, 1985).

In this work, microhemisphere, microcylinder, and planar electrodes are addressed. The differences between the three systems enter the transport equations through the Laplacian operator for the potential Φ and concentration c_i:

$$\nabla^2\Phi = \frac{\partial^2\Phi}{\partial r^2} + \frac{\gamma}{r}\frac{\partial\Phi}{\partial r} \quad (32)$$

$$\gamma = 0 \text{ planar electrode} \quad (33)$$

$$\gamma = 1 \text{ cylindrical electrode} \quad (34)$$

$$\gamma = 2 \text{ hemispherical electrode} \quad (35)$$

The current density in solution also varies differently with position for the different geometries, Eq. 21,

$$i = i|_{r=a}\left(\frac{a}{r}\right)^\gamma \quad (36)$$

The equations presented in this section form the mathematical model and were solved using Newman's finite-difference algorithm (Newman, 1968, 1973a).

It is important to note that the microhemisphere equations might be used to simulate qualitatively the microdisk system for very small disks (less than 5 μm dia.). It is commonly stated that the two systems are quite different in that the hemisphere maintains a uniform reaction rate over its surface, while the disk has a nonuniform reaction distribution. For this reason, it has been stated in numerous publications that the two systems can never be described quantitatively by the same differential equations. Inspection of the diffusion-limited current density (i_{lim}) expressions for disk and hemisphere:

$$i_{lim} = \frac{4}{\pi}\frac{nFDc^\infty}{a_{disk}} \quad (37)$$

$$i_{lim} = \frac{nFDc^\infty}{a_{hemisphere}} \quad (38)$$

and the current density under primary current distribution conditions (Newman, 1966a) (i.e., no kinetic or mass-transport resistance):

$$i = \frac{4}{\pi}\frac{\kappa\Phi_o}{a_{disk}} \quad (39)$$

$$i = \frac{\kappa\Phi_o}{a_{hemisphere}} \quad (40)$$

illustrates that the substitution of

$$a_{disk} = \frac{\pi}{4}a_{hemisphere} \quad (41)$$

might be used to simulate the disk system using the hemisphere equations. This would simplify considerably the two-dimensional analysis of the disk system since the one-dimensional equations for the hemisphere are much more easily solved.

Results and Discussion

Experimentally obtained voltammograms for Ga deposition from the 40:60 melt are shown in Figure 3. A 12.5 μm radius Pt

wire was employed as the working electrode, and an aluminum wire was used as the reference. Cathodic currents are reported as negative values. We will not address the anodic portions of the voltammograms. It is clear from an inspection of Figure 3 that mass-transport resistance is significant for potentials negative to −0.75 V, as faster sweep rates yielded larger currents. The broad range of nearly zero current (between −0.2 and −0.6 V) indicates a kinetically hindered electrode reaction for the deposition process.

Between −0.5 and −0.7 V, slight oscillations in the current-potential traces of Figure 3 are observed. In an effort to clarify this region, a 10 μm Pt microdisk electrode was employed. Since the area of the microdisk is far less than that of the microcylinder, single events (such as those associated with Ga crystallization phenomena) may not be as obscured by the noise of the other similar events. (There will be less of an averaging of signals.) The microdisk data of Figure 4 clearly show repeated oscillations at the onset and termination of the Ga deposition reaction. The boxed regions of Figure 4 indicate the relevant portions of the current trace. Although we do not address further the oscillation phenomena in this work, it is evident that microdisks can be used to elucidate such behavior.

As mentioned directly below Eq. 31, controlled-current experiments are more useful than controlled-potential experiments for the acquisition of parameters not associated with the electrode reaction. The current step results of Figure 5 were

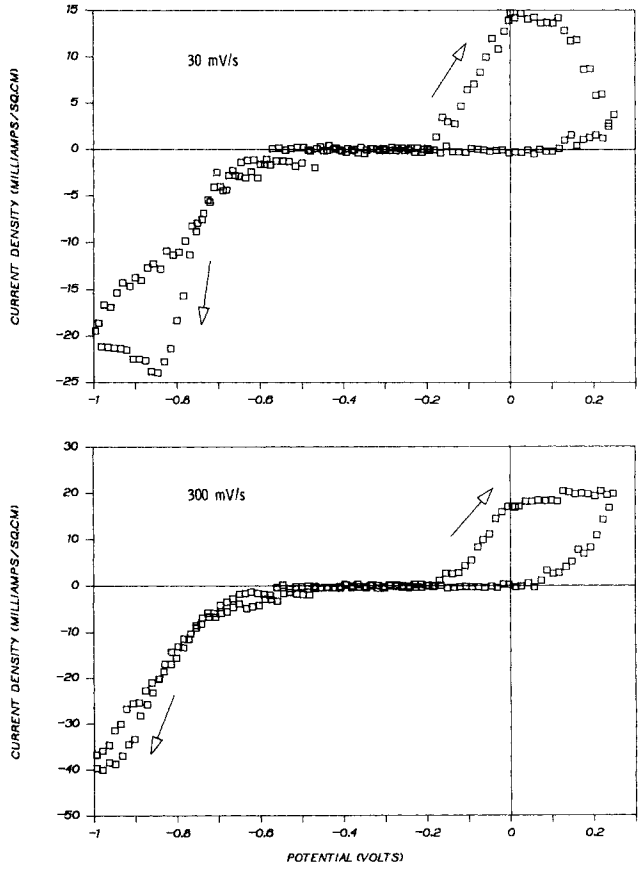

Figure 3. Cyclic voltammogram of 40:60 melt.
Top curve: 30 mV/s.
Bottom curve: 300 mV/s
Working electrode: 12.5 μm radius Pt wire

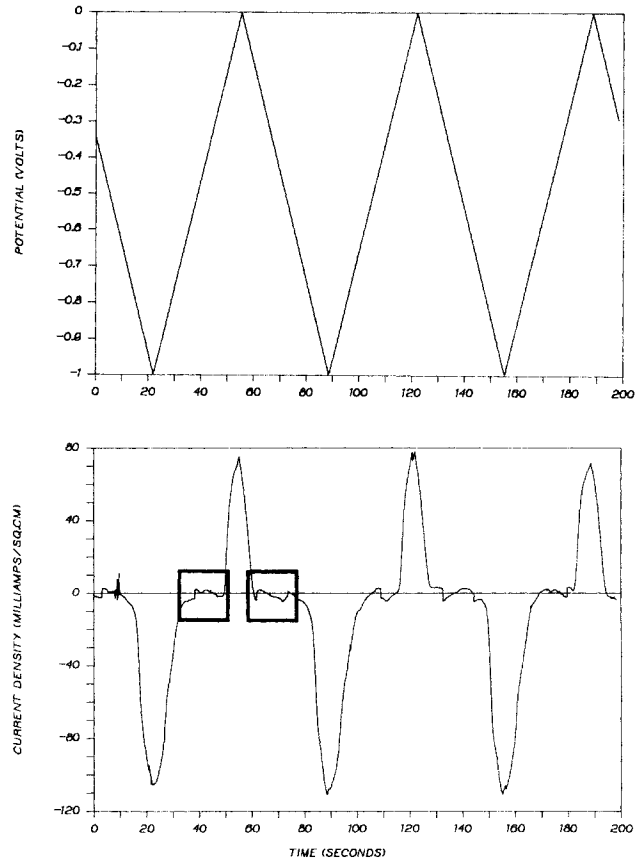

Figure 4. Current oscillations for Ga deposition reaction.
Top curve: Electrode potential
Bottom curve: Current response
Working electrode: 5 μm radius Pt disk

used to obtain K_{III}, k_f, and k_b. (The equilibrium constant K_{III} and k_f were fitted to the data, and Eq. 5 was used to extract k_b.) The diffusion coefficients of $GaCl_4^-$, $Ga_2Cl_7^-$, and Cl^- were set to 1×10^{-7} cm^2/s in accordance with data for the $AlCl_3$–ImCl system (Lai and Skyllas-Kazacos, 1988; Carpio et al., 1979; Hussey et al., 1979). A value of 1×10^{-8} cm^2/s was used for the larger Im^+ ion. (The model is not particularly sensitive to the Im^+ diffusion coefficient.) Shown in Figure 5 are data for a 14.1 mA/cm^2 current step. Data for a 17.7 mA/cm^2 current step were quite similar and are not shown. The two experiments were modeled by the microcylinder equations presented; good agreement was obtained with the following parameter values:

$$K_{III} = 0.30$$

$$k_f = 0.010 \text{ cm}^3/\text{mol} \cdot \text{s}$$

$$k_b = 0.033 \text{ cm}^3/\text{mol} \cdot \text{s}$$

The transition time corresponds to the concentration of $Ga_2Cl_7^-$, obtaining a value of nearly zero at the electrode surface, at which time the potential is driven to a more negative (cathodic) value since another electrode reaction is forced to occur. The transition time in Figure 5 is 24 s. For the 17.7 mA/cm^2 experiment, a transition time of 16 s was observed. Results of the model for the 17.7 mA/cm^2 current step are shown in Figure 6. The dimensionless surface concentration of $Ga_2Cl_7^-$ (c_3/c_3^∞) is

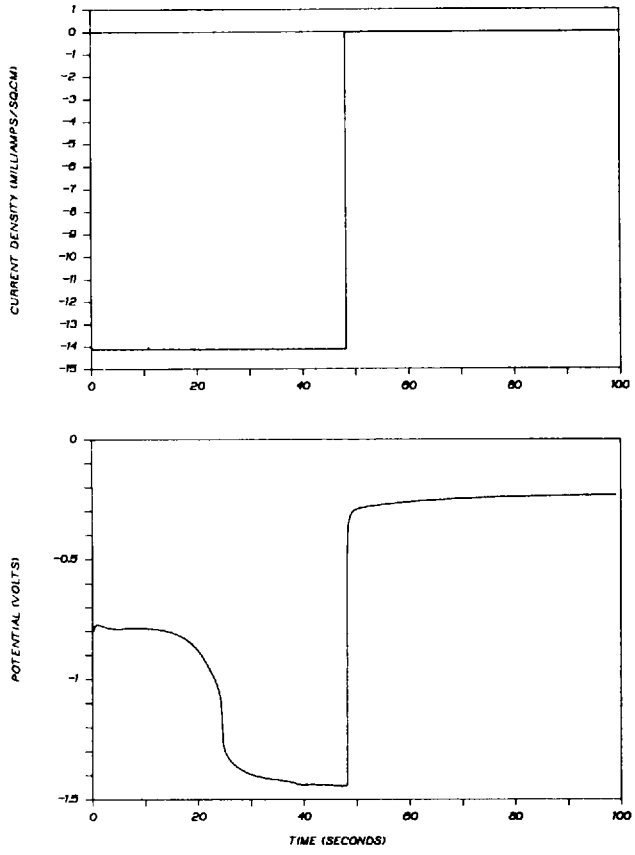

Figure 5. Current-step experiment.
Top curve: Current source
Bottom curve: Potential response
Working electrode: 12.5 μm radius Pt wire
A 24 s transition time is observed; open-circuit potential is shown to be −238 mV

plotted against dimensionless time (tD_3/a^2) and position ($(r - a)/(5a)$). Far from the electrode (dimensionless position of 1), the $Ga_2Cl_7^-$ concentration maintains its bulk value for all times. At the electrode surface (dimensionless position of 0), the $Ga_2Cl_7^-$ concentration is initially that of the bulk and reaches a value of zero near a dimensionless time of unity. The current is switched to a value of zero soon after the transition time, and the surface concentration of $Ga_2Cl_7^-$ is then augmented by transport from the bulk to the surface.

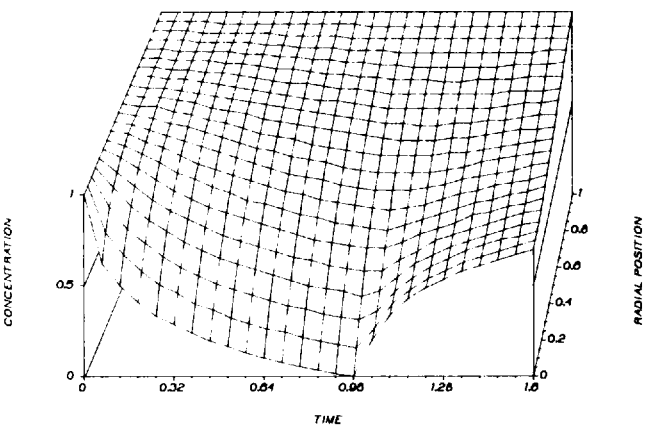

Figure 6. Simulated $Ga_2Cl_7^-$ concentration profile for 17.7 mA/cm² current-step experiment.
Dimensionless concentration: c_3/c_3^∞.
Dimensionless position: $(r - a)/(5a)$.
Dimensionless time: tD_3/a^2

The open-circuit potential of Figure 5 can be used to extract U^o, Eq. 12:

$$V = U^o + \frac{RT}{nF} \ln \frac{c_3^\infty}{c_2^\infty (c_4^\infty)^3} \text{ (open circuit)} \qquad (42)$$

A value of −0.33 V was obtained for U^o. (The concentration terms in Eq. 42 account for the deviation from the −0.238 V observed for the open-circuit potential of Figure 5. In general, the open-circuit potential is very reproducible in this system.) It should be noted that if the homogeneous reaction forming $Ga_2Cl_7^-$, Eq. 3, were assumed to be in equilibrium, then no limiting current would be observed (and no transition time either) for the system as long as $GaCl_4^-$ was present. Since transition times and limiting currents are observed for the Ga and Al systems, there must be some kinetic hinderance to the dimerization reaction. With regard to the present work, a value of k_f much larger than that which was obtained would yield increasing surface concentrations of $Ga_2Cl_7^-$ during deposition. This can be rationalized by inspection of Eq. 7 (replacing Al species with Ga species). For every four moles of $Ga_2Cl_7^-$ reduced, seven moles of $GaCl_4^-$ are produced, which through the homogeneous equilibrium would produce more $Ga_2Cl_7^-$.

The electrode reaction was investigated by means of linear-sweep voltammetry. The potential region of interest for the deposition reaction extends from −0.2 to −0.8 V, as exhibited in Figure 3. Shown in Figure 7 are potential sweep data (300 mV/s) used to obtain electrode kinetic parameters. The dashed line in Figure 7 corresponds to the model calculations with the following electrode kinetic parameters:

$$i_{o,\infty} = 0.010 \text{ mA/cm}^2$$
$$\beta = 0.11$$

where the subscript ∞ denotes that the exchange current density of 0.010 mA/cm² is based on bulk concentrations, Eq. 13. It is interesting to note that MacArthur and Bendert (1986) found

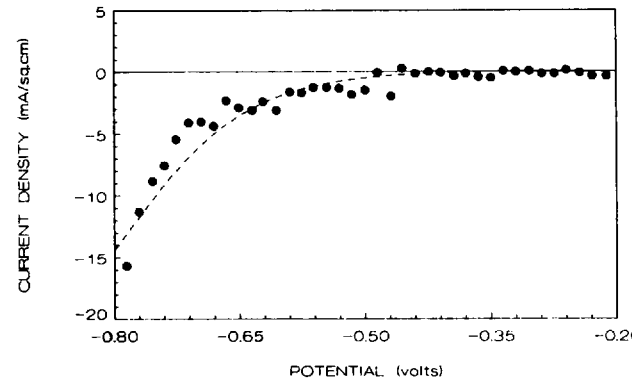

Figure 7. (—) Potential-sweep experiment, 30 mV/s.
Working electrode: 12.5 μm radius Pt wire
• Experimental data; --- model results

values of i_o = 0.2 mA/cm^2 and β = 0.25 for the acidic $AlCl_3$–ImCl system. (β was extracted from their Tafel plots.) In general, it appears that the Ga deposition process from the Ga-based melt, which involves species of higher molecular weight, is more kinetically hindered than the Al deposition process from the analogous Al-based melt.

The utility of microelectrodes for the analysis of the molten salt system is investigated in Figure 8. Shown are simulated voltammograms for the 40:60 melt using the obtained parameters for a planar, a 12.5 μm radius microcylinder, and a 12.5 μm radius microhemisphere electrode. The counterelectrode is located 62.5 μm from the working electrode, and its contour is taken to match that of the working electrode; the 62.5 μm separation corresponds, essentially, to infinity for the cylindrical and hemispherical electrodes. Three trends are immediately identifiable:

1. The current densities increase for specified electrode potentials in the order of planar < microcylinder < microhemisphere;

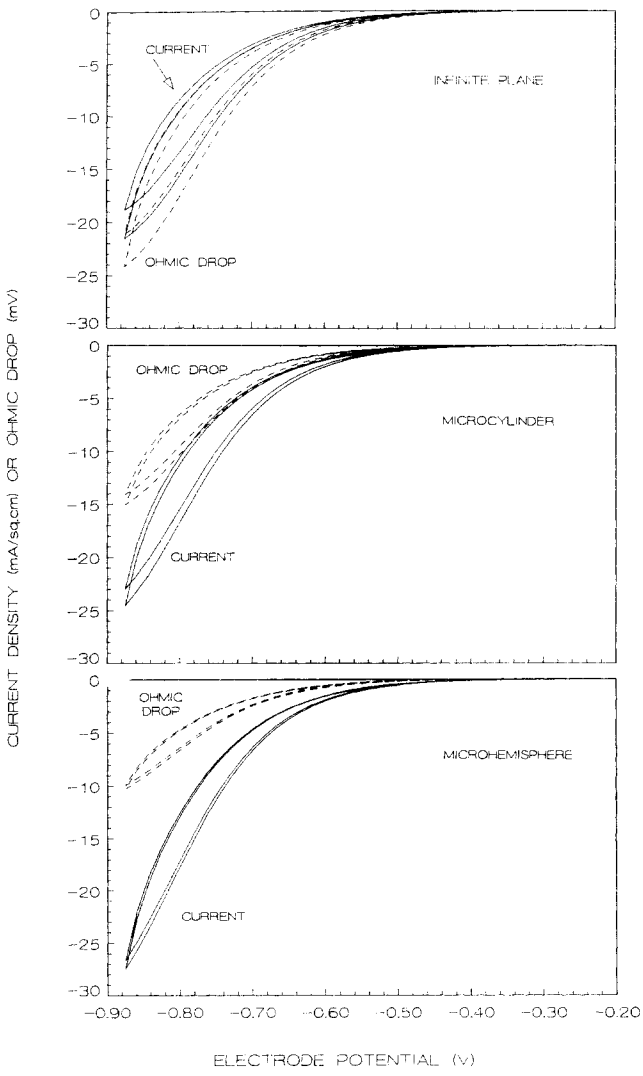

Figure 8. Theoretical comparison of infinite plane, microcylinder, and microdisk (12.5—μm radius) electrodes.
Microcylinder, microdisk radii: 12.5 μm

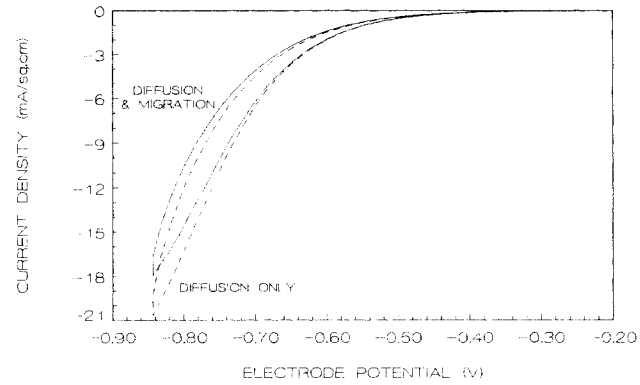

Figure 9. Effect of migration on Ga deposition process.
To obtain *Diffusion Only* curve, migration component for $Ga_2Cl_7^-$ species was set to zero
12.5 μm radius microcylinder used for analysis

2. The ohmic drop decreases in the order of planar > microcylinder > microhemisphere (note that the current densities are not equal for the different systems at various electrode potentials; also, the ohmic potential drop corresponds to Φ_o since the diffusion potential [Newman, 1973a] is very small in these cases);

3. The amount of hystersis follows the order of planar > microcylinder > microhemisphere.

Since the ohmic drop must be subtracted from the measured potential to obtain kinetic parameters, it is clear that the microelectrodes provide a distinct advantage. In addition, the microcylinder and microhemisphere electrodes provide uniform reaction distributions.

The importance of migration for the transport of $Ga_2Cl_7^-$ is shown in the simulated voltammograms of Figure 9. The dashed curve was obtained by setting the $Ga_2Cl_7^-$ migration term to zero. Since the cathode is negative, the $Ga_2Cl_7^-$ anion migration flux is away from the electrode and impedes deposition. Greater than a 10% increase in the current density at −0.85 V is observed if the $Ga_2Cl_7^-$ migration flux is neglected.

Conclusions

Microelectrodes have been shown to be particularly useful for the acquisition of thermodynamic, transport, and kinetic data for the gallium trichloride/1-methyl-3-ethylimidazolium chloride room-temperature molten salt that has been used for the formation of GaAs thin films (Carpenter and Verbrugge, 1989). Physicochemical constants for the Ga deposition process in the chlorogallate melt were obtained using microcylinder electrodes. Migration was found to be an important mode of ionic transport. Microdisk electrodes were employed to investigate oscillation phenomena related possibly to metal crystallization processes. Analysis of the electrode kinetic data indicates that the Ga deposition reaction from the basic chlorogallate melt is not as facile as that of Al deposition from the analogous acidic chloroaluminate melt. The benefits of microelectrodes relative to traditional macroelectrodes (planar electrodes) are elucidated by simulation results.

Acknowledgment

The authors thank R. M. Bendert for preparation of the ImCl and D. M. MacArthur for a number of insightful discussions.

Notation

a = electrode radius, cm
c = concentration, mol/cm^3
D = diffusion coefficient, cm^2/s
$f = F/RT$, mol/V · equiv
F = Faraday's constant, 96,487C/equiv.
i = current density, A/cm^2
i_o = exchange current density of reaction, A/cm^2
k_a = anodic rate constant
k_b = backward rate constant
k_c = cathodic rate constant
k_f = forward rate constant
K = equilibrium constant
n = number of electrons in reaction, equivalents/mol
N = ion flux, mol/cm^2 · s
r = radial position, cm
R = gas constant, 8.314 J/mol · K
t = time, s
T = temperature, K
V = electrode potential relative to reference electrode, V
z = charge number, equivalents/mol

Greek letters

β = symmetry factor of reaction
η_s = surface overpotential of reaction, V
κ = electrolyte conductivity, mho/cm
Φ = electrical potential, V

Subscripts

1 = Im^+
2 = $GaCl_4^-$
3 = $Ga_2Cl_7^-$
4 = Cl^-
i = species i
I = reaction I
II = reaction II
III = reaction III

Literature Cited

Amatore, C. A., M. R. Deakin, and R. M. Wightman, "Electrochemical Kinetics at Microelectrodes. I: Quasi-Reversible Electron Transfer at Cylinders," *J. Electroanal. Chem.*, **206,** 23 (1986).

Amatore, C., B. Fosset, J. Bartelt, M. R. Deakin, and R. M. Wightman, "Electrochemical Kinetics at Microelectrodes: V. Migrational Effects on Steady or Quasi-Steady-State Voltammograms," *J. Electroanal. Chem.*, **256,** 255 (1988).

Aoki, K., and J. Osteryoung, "Diffusion-Controlled Current at the Stationary Finite Disk Electrode," *J. Electroanal. Chem.*, **122,** 19 (1981).

———, "Formulation of the Diffusion-Controlled Current at Very Small Stationary Disk Electrodes," *J. Electroanal. Chem.*, **160,** 335 (1984).

Aoki, K., K. Akimoto, K. Tokuda, H. Matsuda, and J. Osteryoung, "Linear Sweep Voltammetry at Very Small Stationary Disk Electrodes," *J. Electroanal. Chem.*, **171,** 19 (1984).

Aoki, K., K. Honda, K. Tokuda, and H. Matsuda, "Voltammetry at Microcylinder Electrodes. I, II, III," *J. Electroanal. Chem.*, **182,** 267; **186,** 79; **195,** 51 (1985).

Bamford, C. H., and R. G. Compton, eds. *Electrode Kinetics: Principles and Methodology,* Comprehensive Chemical Kinetics, vol. 26 Elsevier, Amsterdam (1986).

Bard, A. J., and L. R. Faulkner, *Electrochemical Methods,* Wiley, New York, 501 (1980).

Bond, A. M., K. B. Oldham, and C. G. Zoski, "Theory of Electrochemical Processes at an Inlaid Disc Microelectrode Under Steady-State Conditions," *J. Electroanal. Chem.*, **245,** 71 (1988).

Carlin, R. T., and R. A. Osteryoung, "Microelectrodes in the Examination of Anodic and Cathodic Limit Reactions of an Ambient Temperature Molten Salt," *J. Electroanal. Chem.*, **252,** 81 (1988).

Carpenter, M. K., and M. W. Verbrugge, "Electrochemical Codeposition of Gallium Arsenic from a Room-Temperature Chlorogallate Melt," *J. Electrochem. Soc.*, **137,** 123 (1990).

Carpio, R. A., L. A. King, R. E. Lindstrom, J. C. Nardi, and C. L. Hussey, "Density, Electric Conductivity, and Viscosity of Several *N*-Alkylpyridinium Halides and Their Mixtures with Aluminum Chloride," *J. Electrochem. Soc.*, **126,** 1644 (1979).

Carslaw, H. S., and J. C. Jaeger, *Conduction of Heat in Solids,* Oxford Univ. Press. London (1959).

Conte, S. D., and C. de Boor, *Elementary Numerical Analysis,* 3d ed., McGraw-Hill, New York (1980).

Flanagan, J. B., and L. Marcoux, "Digital Simulation of Edge Effects at Planar Disk Electrodes," *J. Phys, Chem.*, **77,** 1051 (1973).

Fleischmann, M., and S. Pons, "The Behavior of Microdisk and Microring Electrodes. Mass Transport to the Disk in the Unsteady State, Chronopotentiometry," *J. Electroanal. Chem.*, **250,** 257 (1988).

Fleischmann, M., S. Pons, D. Rolison, and P. Schmidt, *Ultramicroelectrodes,* Datatech Science, Morganton, NC (1987).

Fleischmann, M., J. Daschbach, S. Pons, "The Behavior of Microdisk and Microring Electrodes. Application of Neuman's Integral Theorm to the Prediction of the Steady-State Response of Microdisks," *J. Electroanal. Chem.*, **263,** 189 (1989).

Frensley, W. R., "Gallium Arsenide Transistors," *Scientific American,* **257,** 80 (1987).

Heinze, J., "Diffusion Processes at Finite (Micro) Disk Electrodes Solved by Digital Simulation," *J. Electroanal. Chem.*, **124,** 73 (1981).

Hirschfelder, J. O., C. F. Curtiss, and R. B. Bird, *Molecular Theory of Gases and Liquids,* Wiley, New York, 11, esp. pp. 712–720 (1954).

Howell, J. O., *Current Separations,* Product literature of Bioanalytical Systems, West Lafayette, IN (July 1987).

Hussey, C. L., "Room-Temperature Molten Salt Systems," *Adv. Molten Salt Chem.*, **5,** 185 (1983).

Hussey, C. L., L. A. King, and J. S. Wilkes, "An Electrochemical Study of the Fe(III)/Fe(II) Electrode Reaction in the Aluminum Chloride + *N*-(*N*-Butyl)Pyridinium Chloride Molten Salt System," *J. Electroanal. Chem.*, **102,** 321 (1979).

Hussey, C. L., T. B. Scheffler, J. S. Wilkes, and A. A. Fannin, Jr., "Chloroaluminate Equilibria in the Aluminum Chloride-1-Methyl-3-Ethylimidazolium Chloride Ionic Liquid," *J. Electrochem. Soc.*, **133,** 1389 (1986).

Kovach, P. M., W. L. Caudill, D. G. Peters, and R. M. Wightman, "Faradaic Electrochemistry at Microcylinder, Band, and Tubular Band Electrodes," *J. Electroanal. Chem.*, **185,** 285 (1985).

Lai, P. K., and M. Skyllas-Kazacos, "Electrodeposition of Aluminum in Aluminum Chloride/1-Methyl-3-Ethylimidazolium Chloride," *J. Electroanal. Chem.*, **248,** 431 (1988).

MacArthur, D. M., and R. M. Bendert, "The Aluminum Electrode in 1-Ethyl, 3-Methylimidazolium Chloride/Aluminum Trichloride Liquid Electrolytes," EC-689, paper given at Electrochem. Soc. Meet, (May 4–9, 1986).

Nanis, L., and W. Kesselman, "Engineering Applications of Current and Potential Distributions in Disk Electrode Systems," *J. Electrochem. Soc.*, **118,** 454 (1971).

Newman, J., "Resistance for Flow of Current to a Disk," *J. Electrochem. Soc.*, **113,** 501 (1966).

———, "Current Distribution on a Rotating Disk below the Limiting Current," *J. Electrochem. Soc.*, **113,** 1235 (1966b); see also **114,** 239 (1967).

———, "Numerical Solution of Coupled, Ordinary Differential Equations," *Ind. Eng. Chem. Fundam.*, **7,** 514 (1968).

———, *Electrochemical Systems,* Prentice-Hall, Englewood Cliffs, NJ (1973a).

———, "The Fundamental Principles of Current Distribution and Mass Transport in Electrochemical Cells," *Electroanalytical Chemistry, A Series of Advances,* A. J. Bard, ed., Dekker, New York, 326–329 (1973b).

Oldham, K. B., "Edge Effects in Semiinfinite Diffusion," *J. Electroanal. Chem.*, **122,** 1 (1981).

Stephens, M. M., and E. D. Moorhead, "An Examination of the Finite-Difference Numerical Approach to the Solution of Electrochemically Induced Diffusive Transport at Stationary Solid Cylinder Electrodes. Single Sweep Voltammetry of Reversible Systems," *J. Electroanal. Chem.*, **164,** 17 (1984).

Sujaritvanichpong, S., K. Aoki, K. Tokuda, and H. Matsuda, "Voltam-

metry at Microcylinder Electrodes. IV: Normal and Differential Pulse Voltammetry," *J. Electroanal. Chem.*, **199,** 271 (1986).
Verbrugge, M. W., and C. W. Tobias, "Triangular Current-Sweep Chronopotentiometry at Rotating Disk and Stationary, Planar Electrodes," *J. Electroanal. Chem.*, **196,** 243 (1985).
Watson, G. N., *A Treatise on the Theory of Bessel Functions,* Cambridge Univ. Press, London (1952). (For classical integral-transform works concerning the disk system, see ch. 14.3 for Neumann's integral theorm and ch. 13.4 for the results of Weber, Sonine, and Schafheitlin.)
Wicelinski, S. P., and R. J. Gale, "Gallium Species Electrochemistry in Room Temperature Chloroaluminate Melts," Electrochem. Soc. Meet., Honolulu, Oct. 18–23, Abstract 1495 (1987).
Wicelinski, S. P., R. J. Gale, and J. S. Wilkes, "Low-Temperature Chlorogallate Molten Salt Systems," *J. Electrochem. Soc.*, **134,** 262 (1987).
Wightman, R. M., "Microvoltammetric Electrodes," *Anal. Chem.*, **53,** 1125A (1981).

Manuscript received Jan. 8, 1990, and revision received Apr. 9, 1990.